Table 1. Binding affinities (nM) to S1P receptors.

	$S1P_1$	$S1P_2$	$S1P_3$	$S1P_4$	$S1P_5$
S1P	0.47 ± 0.34	0.31 ± 0.02	0.17 ± 0.05	95 ± 25	0.61 ± 0.39
Compound A	0.21 ± 0.17	>10,000	5.0 ± 2.7	5.9 ± 2.3	0.59 ± 0.27
FTY720	300 ± 51	>10,000	>10,000	>5000	2623 ± 317

IC_{50} measurements determined by competition of $S1^{33}P$ binding to membranes prepared from stably transfected CHO cells expressing the indicated S1P receptor (*7*).

ed specific S1P receptor agonism rather than off-target effects. The correlation between phosphorylation and induction of lymphopenia is supported by studies on structural analogs of FTY720, in which the *R* isomer of 2-amino-4-(4-heptyloxyphenyl)-2-methylbutanol was reported to be active in a T cell depletion assay and immunosuppressive in a lymph node gain model in rats, while the *S* isomer was inactive (*16*). We synthesized the enantiomers and found that the active species was readily phosphorylated by rat blood (4.58-fold better than FTY720) and was fully efficacious at depleting lymphocytes in mice at 0.2 mg/kg, whereas the other enantiomer showed only trace phosphorylation in rat blood and was inactive at 1 mg/kg (*8*).

Quantitation of lymphocytes in thoracic duct lymph (TDL) from cannulated rats (Fig. 4B) showed that decreases in peripheral blood lymphocytes induced by S1P or Compound A were temporally associated with, or were slightly preceded by, a rapid decline in thoracic duct lymphocytes, as was seen for FTY720 (*15*). The duration of TDL lymphopenia was longer for the synthetic compounds than for S1P, correlating with compound levels in both blood and lymph (*8*). S1P, delivered by continuous infusion to avoid adverse cardiovascular effects, induced both blood lymphopenia and depletion of lymphocytes from TDL.

FTY720 has been shown to sequester cells in lymph node and not spleen (*14*). Our data in mouse and rat with Compound B show that the same pattern of sequestration was achieved with nonhydrolyzable phosphonate derivatives (*7*). Lymphocyte sequestration induced by S1P receptor agonists was observed histologically within 3 hours after a single dose. Mesenteric nodes showed disappearance of lymphocytes from subcapsular and medullary sinuses, with the logjamming of lymphocytes on the abluminal side of sinus lining endothelium (Fig. 5).

Lipid receptors may have a broad role in regulating immune responses. Although deletion of the G protein–coupled receptor for lysophosphatidylcholine (G2A) altered lymphoid organ structure and caused autoimmunity (*17*), pharmacological agonism of S1P receptors shown here causes immunosuppression. The precise role of individual S1P receptors and the hierarchy of their contributions to lymphocyte sequestration in SLO remain to be clarified, because S1P receptors are expressed on both endothelium and lymphocytes. S1P alters junctional properties of endothelium (*18, 19*). The role of the S1P receptor is separable from CCR7-dependent events because the sequestration of lymphocytes still occurred in the CCR7-deletant mice upon FTY720 treatment as shown by Henning *et al.* (*20*).

Regulation of lymphocyte trafficking through lymph node may be a physiological function of S1P, a lysosphingolipid implicated in regulating cardiac (*21, 22*) and pressor functions (*23*). Exposure to free S1P is regulated by protein and lipid binding factors in blood (*24*) and by phosphatase activities (*25*), that limit systemic side effects of S1P exposure. Regulation of blood lymphocyte numbers by systemic S1P receptor agonism may thus allow clinically useful immunosuppression through lymphocyte sequestration.

References and Notes

1. J. L. Gowans, *Immunol. Today* **17**, 288 (1996).
2. E. C. Butcher, M. Williams, K. Youngman, L. Rott, M. Briskin, *Adv. Immunol.* **72**, 209 (1999).
3. K. M. Ansel, J. G. Cyster, *Curr. Opin. Immunol.* **13**, 172 (2001).
4. V. Brinkmann, D. D. Pinschewer, L. Feng, S. Chen, *Transplantation* **72**, 764 (2001).
5. V. Brinkmann, D. Pinschewer, K. Chiba, L. Feng, *Trends Pharmacol. Sci.* **21**, 49 (2000).
6. H. H. Neumayer *et al.*, *Transplantation* **67**, S204 (1999).
7. Supplemental material is available on *Science* Online at www.sciencemag.org/cgi/content/full/1070238/DC1.
8. S. Mandala, J. Bergstrom, R. Hajdu, data not shown.
9. J. K. Chen, W. S. Lane, S. L. Schreiber, *Chem. Biol.* **6**, 221 (1999)
10. M. H. Graeler, G. Bernhardt, M. Lipp, *Curr. Top. Microbiol. Immunol.* **246**, 131 (1999).
11. T. Hla, M.-J. Lee, N. Ancellin, J. H. Paik, M. J. Kluk, *Science* **294**, 1875 (2001).
12. N. Fukushima, I. Ishii, J. J. A. Contos, J. A. Weiner, J. Chun, *Annu. Rev. Pharmacol. Toxicol.* **41**, 507 (2001).
13. I. Ishi *et al.*, *J. Biol. Chem.* **276**, 33697 (2001).
14. Z. J. Luo, T. Tanaka, F. Kimura, M. Miyasaka, *Immunopharmacology* **41**, 199 (1999).
15. K. Chiba *et al.*, *J. Immunol.* **160**, 5037 (1998).
16. M. Kiuchi *et al.*, *J. Med. Chem.* **43**, 2946 (2000).
17. J. H. Kabarowski, K. Zhu, L. Q. Le, O. N. Witte, Y. Xu, *Science* **293**, 702 (2001).
18. M.-J. Lee *et al.*, *Cell* **99**, 301 (1999).
19. J. G. N. Garcia *et al.*, *J. Clin. Invest.* **108**, 689 (2001).
20. G. Henning *et al.*, *J. Exp. Med.* **194**, 1875 (2001).
21. K. Liliom *et al.*, *Biochem. J.* **355**, 189 (2001).
22. A. Sugiyama, Y. Yatomi, Y. Ozaki, K. Hashimoto, *Cardiovasc. Res.* **46**, 119 (2000).
23. A. Sugiyama, N. N. Aye, Y. Yatomi, Y. Ozaki, K. Hashimoto, *Jpn. J. Pharmacol.* **82**, 338 (2000).
24. N. Murata *et al.*, *Biochem. J.* **352**, 809 (2000).
25. S. M. Mandala *et al.*, *Proc. Natl. Acad. Sci. U.S.A.* **97**, 7859 (2000).

26. Acknowledgments are presented in (*7*).

25 January 2002; accepted 8 March 2002
Published online 28 March 2002;
10.1126/science.1070238
Include this information when citing this paper.

Regulation of Mitochondrial Biogenesis in Skeletal Muscle by CaMK

Hai Wu,[1] Shane B. Kanatous,[1] Frederick A. Thurmond,[1] Teresa Gallardo,[1] Eiji Isotani,[2] Rhonda Bassel-Duby,[1] R. Sanders Williams[3]*

Endurance exercise training promotes mitochondrial biogenesis in skeletal muscle and enhances muscle oxidative capacity, but the signaling mechanisms involved are poorly understood. To investigate this adaptive process, we generated transgenic mice that selectively express in skeletal muscle a constitutively active form of calcium/calmodulin–dependent protein kinase IV (CaMKIV*). Skeletal muscles from these mice showed augmented mitochondrial DNA replication and mitochondrial biogenesis, up-regulation of mitochondrial enzymes involved in fatty acid metabolism and electron transport, and reduced susceptibility to fatigue during repetitive contractions. CaMK induced expression of peroxisome proliferator-activated receptor γ coactivator 1 (PGC-1), a master regulator of mitochondrial biogenesis in vivo, and activated the PGC-1 gene promoter in cultured myocytes. Thus, a calcium-regulated signaling pathway controls mitochondrial biogenesis in mammalian cells.

The oxidative capacity of specialized myofibers in mammalian skeletal muscles can vary over an order of magnitude, thereby matching metabolic capabilities to different physiologic demands (*1*). The maximum catalytic capacity of mitochondrial enzymes involved in the tricarboxylic

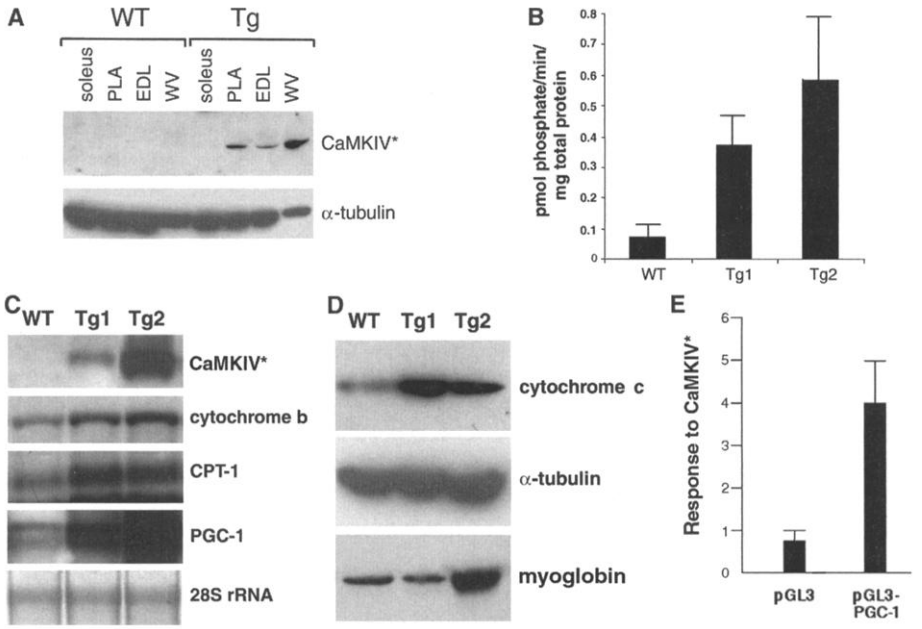

Fig. 1. (**A**) Immunoblot shows CaMKIV* protein expression in subset of skeletal muscles. Protein extracts from soleus, plantaris (PLA), extensor digitorum longus (EDL), and white vastus (WV) muscles harvested from transgenic (Tg) and wild-type (WT) mice were immunoblotted with antibodies to CaMKIV or tubulin and were visualized with an enhanced chemiluminescence reagent (Amersham). Tubulin provides a control for protein loading. (**B**) Activity assay for constitutively active CaMKIV. Protein G–agarose and antibody to CaMKIV were added into dialyzed protein extracts from plantaris muscles of wild-type or two independent transgenic mouse lines (Tg1, Tg2). The immunoprecipitated CaMKIV complexes were incubated with [γ-^{32}P]adenosine triphosphate and used to measure kinase activity toward a CaMKIV-specific peptide substrate (BioMol) in the presence of 1 mM EGTA to inhibit any endogenous CaMK activity. Radioactivity incorporation was measured and used to calculate CaMKIV activity (pmol of phosphate/min per mg of total protein) in muscle extracts. Calculations were made by subtracting activity of samples without added substrate. Histograms represent means ± SEM of three independent assays. (**C**) Northern blot analysis using total RNA (20 μg) from plantaris muscle of wild-type and two independent CaMKIV* transgenic lines (Tg1, Tg2) shows induction of cytochrome b (encoded in mitochondrial DNA) and carnitine palmitoyltransferase-1 (CPT-1) (encoded in nuclear DNA) by overexpression of CaMKIV*. Expression of *PGC-1*, a master regulator of mitochondrial biogenesis, also is increased in CaMKIV* transgenic mice. Ethidium bromide–stained ribosomal RNA serves as a loading control. (**D**) Immunoblot using 50 μg of protein extracts from white vastus muscle of wild-type and CaMKIV* transgenic (Tg1, Tg2) mice. Cytochrome c, a nuclear encoded mitochondrial protein, is induced by CaMKIV*. (**E**) A 3-kb proximal promoter region from the human *PGC-1* gene (GenBank accession number AC092834, nucleotide positions 112,379 to 115,388), linked to a luciferase reporter gene in the plasmid vector pGL3, is activated by CaMKIV* in C2C12 myogenic cells. Cells were harvested 36 hours after transfection, and luciferase activity was assayed with the Luciferase Assay System (Promega). Response values shown are relative to promoter activity in the absence of CaMKIV*. All results were corrected for variations in transfection efficiency by normalization to expression of a cotransfected pCMV-LacZ plasmid. Histograms represent means ± SEM of three independent transfections.

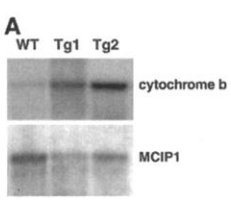

Fig. 2. CaMKIV* increases mitochondrial DNA replication and mitochondrial biogenesis. (**A**) Southern blot analysis of mitochondrial and genomic DNA. Total cellular DNA (20 μg) isolated from gastrocnemius muscles of wild-type and two independent CaMKIV* transgenic lines (Tg1, Tg2) was digested with Nco I and subjected to Southern blot analysis using cytochrome b cDNA, a probe for mitochondrial DNA, or *MCIP1* cDNA, a nuclear-encoded gene. (**B**) Transmission electron microscopy of plantaris muscle sections from wild-type (WT) and CaMKIV* transgenic mice (TG). Thickness of representative subsarcolemmal mitochondrial clusters is highlighted with a line. Scale bar, 100 nm.

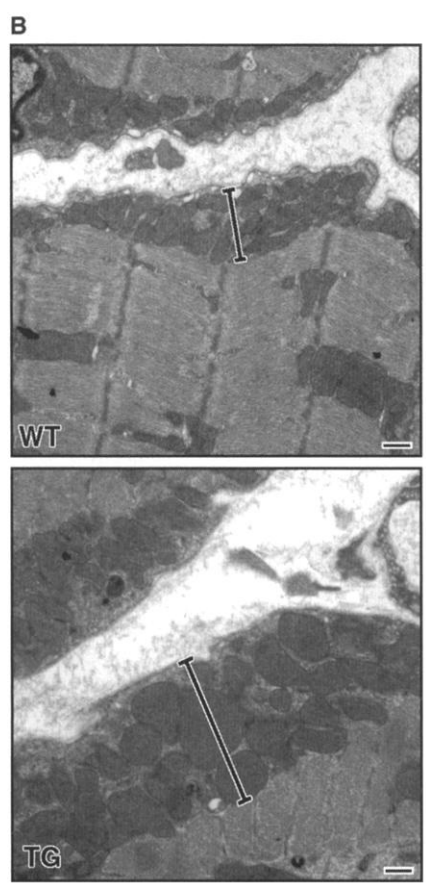

acid cycle or in the electron transport chain is a determining factor for muscle oxidative capacity and resistance to fatigue (*2*). Both long-term endurance exercise training and chronic low-frequency motor nerve pacing promote mitochondrial biogenesis and enhance muscle oxidative capacity (*3, 4*). Increased muscle use also promotes transformation of specialized myofiber subtypes (*5*) as a result of transcriptional switching among genes encoding different isoforms of muscle proteins. The molecular signals that drive mitochondrial biogenesis as a component of myofiber adaptation to increased muscle usage are not fully understood.

Chronic electrical stimulation of skeletal muscles results in sustained elevation of intracellular free calcium concentration to a range of 100 to 300 nM, an amplitude sufficient to activate a subset of calcium-regulated enzymes such as calcineurin and CaMK (*6–8*). Calcineurin is involved in the control of skeletal myofiber specialization and can transform type II fibers into type I fibers in a dose-dependent

[1]Departments of Internal Medicine and Molecular Biology, [2]Department of Physiology, University of Texas Southwestern Medical Center, Dallas, TX 75390, USA. [3]Duke University Medical Center School of Medicine, Durham, NC 27710, USA.

*To whom correspondence should be addressed. E-mail: rswilliams@mc.duke.edu

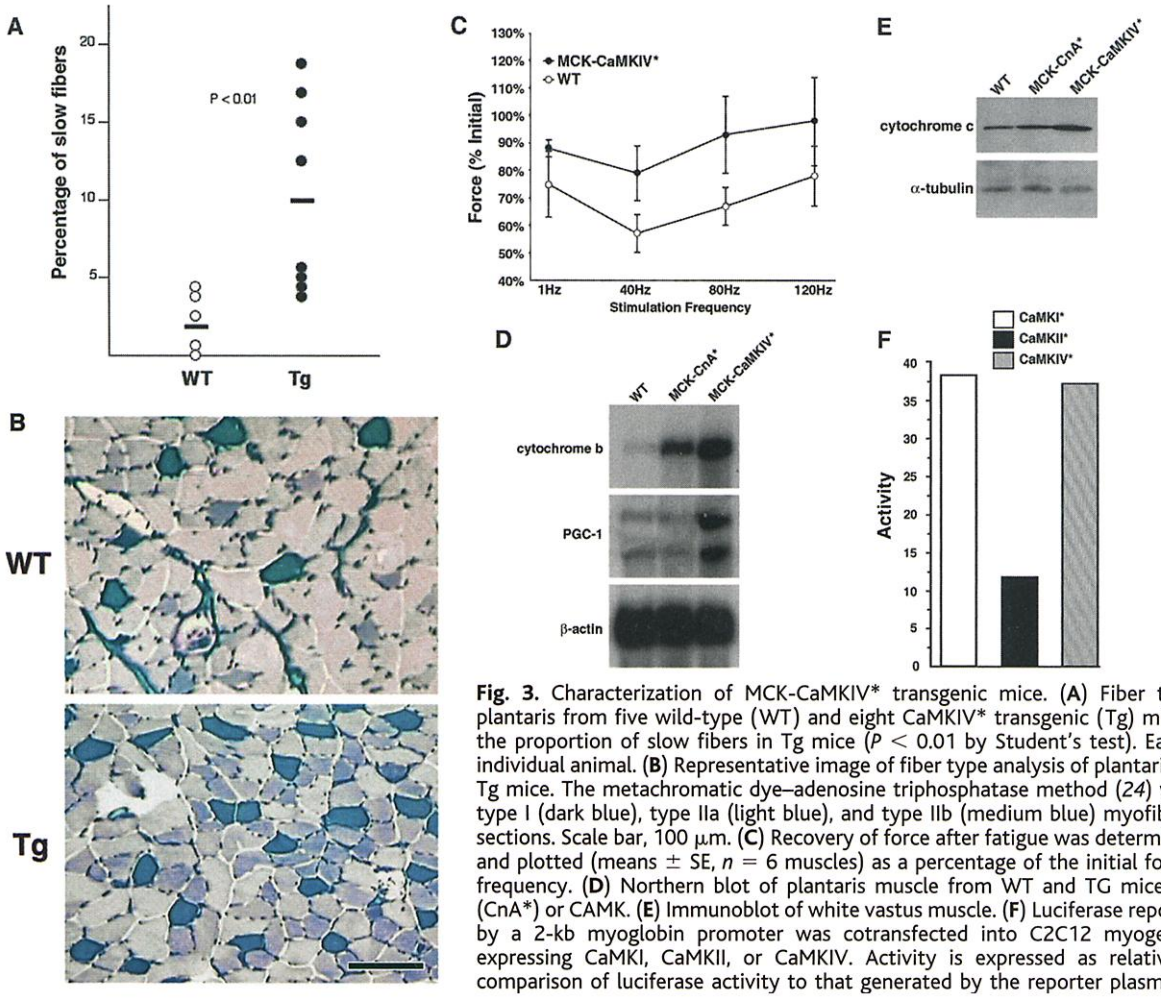

Fig. 3. Characterization of MCK-CaMKIV* transgenic mice. (**A**) Fiber typing analyses of the plantaris from five wild-type (WT) and eight CaMKIV* transgenic (Tg) mice show an increase in the proportion of slow fibers in Tg mice ($P < 0.01$ by Student's test). Each circle represents an individual animal. (**B**) Representative image of fiber type analysis of plantaris muscles from WT and Tg mice. The metachromatic dye–adenosine triphosphatase method (*24*) was used to distinguish type I (dark blue), type IIa (light blue), and type IIb (medium blue) myofibers in plantaris muscle sections. Scale bar, 100 μm. (**C**) Recovery of force after fatigue was determined for the EDL muscle and plotted (means ± SE, $n = 6$ muscles) as a percentage of the initial force at each stimulation frequency. (**D**) Northern blot of plantaris muscle from WT and TG mice expressing calcineurin (CnA*) or CAMK. (**E**) Immunoblot of white vastus muscle. (**F**) Luciferase reporter plasmid controlled by a 2-kb myoglobin promoter was cotransfected into C2C12 myogenic cells with vectors expressing CaMKI, CaMKII, or CaMKIV. Activity is expressed as relative induction based on comparison of luciferase activity to that generated by the reporter plasmid alone.

manner (*6, 9, 10*), and CaMK acts synergistically with calcineurin to activate slow and oxidative fiber-specific gene expression in cultured myocytes (*9*). However, mitochondrial biogenesis can be modulated in skeletal muscles independently of fiber type transformation (*11*), which suggests that distinct signaling mechanisms may be involved.

To examine the relevance of CaMK signaling pathways to fiber type control and mitochondrial biogenesis in intact muscles, we generated transgenic mouse lines overexpressing constitutively active CaMKIV (CaMKIV*) in skeletal muscles. A 4.8-kb proximal region from the promoter of the mouse muscle creatine kinase (MCK) gene (*10*), which is preferentially active in adult skeletal muscles, was used to drive transgene expression (*12*). CaMKIV* is a truncated form of CaMKIV lacking the COOH-terminal autoinhibitory domain and the calcium/calmodulin binding domain, and thus does not require calcium or calmodulin for its activation (*13*). Northern blot analysis confirmed the expression of the transgene in adult skeletal muscles (*12*).

Endogenous CaMKIV transcripts, which are longer than the transgene, were detected in brain and testis. Within skeletal muscles, transgene expression was enriched in muscles composed primarily of type II myofibers, such as the plantaris, extensor digitorum longus (EDL), and white vastus (Fig. 1A). Transgene activity was measured by immunoprecipitating CaMKIV* from skeletal muscles of two independent transgenic lines and assaying for kinase activity toward a peptide substrate in the presence of 1 mM EGTA, which inhibited endogenous CaMK activity in the immunocomplex. Both lines displayed constitutively active CaMKIV activity in their skeletal muscles (Fig. 1B).

Global gene expression profiles of skeletal muscles from wild-type and transgenic mice were compared using DNA microarray technology. NADH (reduced form of nicotinamide adenine dinucleotide) dehydrogenase subunits 1, 2, 3, and 6 showed substantial up-regulation (by a factor of 5 to 6) in the plantaris muscles from transgenic mice relative to wild-type littermates (*12*). These NADH dehydrogenase subunits are encoded by the mitochondrial genome and participate in oxidative phosphorylation. Northern and Western blot analyses showed that the expression of other genes encoding mitochondrial proteins also was induced in skeletal muscles of transgenic mice (Fig. 1, C and D). In plantaris muscles, expression of cytochrome b mRNA, carnitine palmitoyltransferase–1 (CPT-1) mRNA, and cytochrome c proteins was increased in two lines of transgenic mice relative to wild-type animals. The coordinated up-regulation of gene products encoded by both nuclear and mitochondrial genomes in CaMK transgenic mice recapitulated responses to chronic motor nerve stimulation or exercise training (*4, 14*).

Peroxisome proliferator-activated receptor γ coactivator 1 (PGC-1) has been identified as a master regulator of mitochondrial biogenesis (*15, 16*) and as an activator of the mitochondrial fatty acid oxidation pathway (*17*). Transgenic mice overexpressing PGC-1 in the heart show an induction of cardiac mitochondrial biogenesis (*18*). PGC-1 controls adaptive thermogenesis through up-regulation of uncoupling proteins in skeletal muscle and brown adipose tissue (BAT). PGC-1 stimulates the expression of NRF (nuclear respiratory factor) and mtTFA (mitochondrial transcriptional factor A) to activate

expression of nuclear and mitochondrial genes encoding mitochondrial proteins, respectively. *PGC-1* mRNA is induced in both BAT and skeletal muscles upon exposure of the animals to low temperature (*16*). The induction of *PGC-1* by cold exposure is mediated through β adrenergic receptors in BAT, but the mechanisms controlling *PGC-1* expression in skeletal muscles are not known.

We observed an increase of *PGC-1* expression in skeletal muscles of CaMKIV* transgenic mice (Fig. 1C). A 3-kb proximal promoter region from the human *PGC-1* gene was activated by a factor of 4 by CaMKIV* in C2C12 myocytes; this result suggests that CaMK signaling can induce PGC-1 gene expression at a transcriptional level (Fig. 1E). CaMKIV activates several transcription factors, such as CREB (cyclic adenosine monophosphate responsive element-binding protein) and MEF2 (myocyte-specific enhancer factor 2) (*13, 19, 20*); identification of the specific transcription factors responsible for the effect of CaMK on transcription of the *PGC-1* gene will require further investigation.

The expression of mitochondrial genes among specialized myofiber subtypes is proportionate to mitochondrial DNA copy number (*1*). Mitochondrial DNA copy number per nuclear genome was increased in skeletal muscles of MCK-CaMKIV* transgenic mice (Fig. 2A). Transmission electron microscopy performed on sections prepared from plantaris muscles of wild-type and MCK-CaMKIV* transgenic mice revealed that the mitochondria of oxidative myocytes of control plantaris occupied 24 ± 4% of the total cross-sectional area of the myocyte, whereas in MCK-CaMKIV* plantaris this value was 38 ± 6% ($P < 0.05$). The average thickness of subsarcolemmal mitochondrial collections was significantly higher in the MCK-CaMKIV* plantaris than in control plantaris (1.5 ± 0.4 μm versus 1.0 ± 0.1 μm; $P < 0.05$), as assessed from analysis of at least 200 separate muscle fibers from each group (Fig. 2B).

In wild-type mice (F3 hybrid C57BL/6 × SJL), the average percentage of type I fibers in plantaris muscle was about 2%, whereas in MCK-CaMKIV* transgenic mice, type I fibers accounted for about 10% of the total fibers (Fig. 3, A and B). The changes in gene expression and muscle ultrastructure that occurred as consequence of CaMK activity were accompanied by improved contractile performance (fatigue resistance) during repetitive contractions of isolated muscle (EDL) preparations (*21*) (Fig. 3C).

The ability of the CaMKIV* transgene to increase the abundance of type I fibers resembles the response to activated calcineurin (*10*). However, the induction of *PGC-1*, increased expression of mitochondrial genes, and increased expression of nuclear genes encoding mitochondrial proteins was much greater in CaMKIV*-transgenic mice than in calcineurin-transgenic animals (Fig. 3, D and E). Endogenous CaMKIV is not highly expressed in skeletal muscles (*12*), but CaMKI is abundant in this tissue (*22, 23*), and constitutively active forms of CaMKI and CaMKIV are equally potent in activating target genes in a skeletal myocyte background (Fig. 3F).

Overall, our data suggest that CaMK mediates contractile activity-dependent gene regulation in muscle tissues and promotes mitochondrial biogenesis. Further studies will be required to identify the specific CaMK isoform and the specific substrates of CaMK responsible for these effects. Habitual patterns of physical activity have profound effects on human performance in athletes, in healthy individuals during normal aging, and in patients with chronic diseases such as congestive heart failure or respiratory insufficiency. Greater understanding of the molecular signaling pathways by which skeletal muscles sense and respond to changing activity patterns by altering programs of gene expression ultimately may promote the development of novel measures to enhance human performance.

References and Notes

1. R. S. Williams, *J. Biol. Chem.* **261**, 12390 (1986).
2. H. Wang, W. R. Hiatt, T. J. Barstow, E. P. Brass, *Eur. J. Appl. Physiol. Occup. Physiol.* **80**, 22 (1999).
3. D. A. Hood, *J. Appl. Physiol.* **90**, 1137 (2001).
4. R. S. Williams, S. Salmons, E. A. Newsholme, R. E. Kaufman, J. Mellor, *J. Biol. Chem.* **261**, 376 (1986).
5. D. Pette, G. Vrbova, *Rev. Physiol. Biochem. Pharmacol.* **120**, 115 (1992).
6. E. R. Chin *et al.*, *Genes Dev.* **12**, 2499 (1998).
7. G. Y. Wu, K. Deisseroth, R. W. Tsien, *Proc. Natl. Acad. Sci. U.S.A.* **98**, 2808 (2001).
8. A. Alevizopoulos, Y. Dusserre, U. Ruegg, N. Mermod, *J. Biol. Chem.* **272**, 23597 (1997).
9. H. Wu *et al.*, *EMBO J.* **19**, 1963 (2000).
10. F. J. Naya *et al.*, *J. Biol. Chem.* **275**, 4545 (2000).
11. S. M. Hughes, M. M. Chi, O. H. Lowry, K. Gundersen, *J. Cell Biol.* **145**, 633 (1999).
12. See supplementary material on *Science* Online at www.sciencemag.org/cgi/content/full/296/5566/349/DC1.
13. R. Passier *et al.*, *J. Clin. Invest.* **105**, 1395 (2000).
14. R. S. Williams, M. Garcia-Moll, J. Mellor, S. Salmons, W. Harlan, *J. Biol. Chem.* **262**, 2764 (1987).
15. P. Puigserver *et al.*, *Cell* **92**, 829 (1998).
16. Z. D. Wu *et al.*, *Cell* **98**, 115 (1999).
17. R. B. Vega, J. M. Huss, D. P. Kelly, *Mol. Cell. Biol.* **20**, 1868 (2000).
18. J. J. Lehman *et al.*, *J. Clin. Invest.* **106**, 847 (2000).
19. H. Bito, K. Deisseroth, R. W. Tsien, *Cell* **87**, 1203 (1996).
20. T. A. McKinsey, C. L. Zhang, J. Lu, E. N. Olson, *Nature* **408**, 106 (2000).
21. R. W. Grange *et al.*, *Am. J. Physiol. Cell. Physiol.* **281**, C1487 (2001).
22. B. Haribabu *et al.*, *EMBO J.* **14**, 3679 (1995).
23. M. R. Picciotto, A. J. Czernik, A. C. Nairn, *J. Biol. Chem.* **268**, 26512 (1993).
24. R. W. Ogilvie, D. L. Feeback, *Stain Technol.* **65**, 231 (1990).

25. We thank D. Kelly and E. N. Olson for critical reading of the manuscript and advice, and J. M. Shelton and C. Humphries for histology and technical assistance. Supported by NIH grants AR40849 and HL06296.

31 October 2001; accepted 11 March 2002

Structure of a Cofactor-Deficient Nitrogenase MoFe Protein

Benedikt Schmid,[1]* Markus W. Ribbe,[4]* Oliver Einsle,[1,3] Mika Yoshida,[1,3] Leonard M. Thomas,[2,3] Dennis R. Dean,[5] Douglas C. Rees,[1,3]† Barbara K. Burgess[4]

One of the most complex biosynthetic processes in metallobiochemistry is the assembly of nitrogenase, the key enzyme in biological nitrogen fixation. We describe here the crystal structure of an iron-molybdenum cofactor–deficient form of the nitrogenase MoFe protein, into which the cofactor is inserted in the final step of MoFe protein assembly. The MoFe protein folds as a heterotetramer containing two copies each of the homologous α and β subunits. In this structure, one of the three α subunit domains exhibits a substantially changed conformation, whereas the rest of the protein remains essentially unchanged. A predominantly positively charged funnel is revealed; this funnel is of sufficient size to accommodate insertion of the negatively charged cofactor.

The two-component enzyme nitrogenase provides the biochemical machinery for the reduction of dinitrogen to ammonia (*1–7*). Biosynthesis of both components, the Fe protein and the MoFe protein, is a complex process, requiring at least 15 different gene products. The MoFe protein (*8*), an $\alpha_2\beta_2$ tetramer, contains in each αβ half two complex metal clusters that are unique in biology and that have yet to be chemically synthesized. One, designated the P cluster, is an [8Fe-7S] cluster that is coordinated by six Cys ligands and bridges the α and β subunits. The other, designated FeMo cofactor (FeMoco), is a [Mo-7Fe-9S] cluster that also contains an endogenous organic component (homocitrate) and is connected to the protein by only two ligands, a Cys and a His, located within the α subunit. The FeMoco represents the site of substrate binding and reduction. In the cell,